NANO LETTERS

pubs.acs.org/NanoLett Letter

Atomic Evolution Mechanism and Suppression of Edge Threading Dislocations in Nitride Remote Heteroepitaxy

Bo Shi,[▽] Zhetong Liu,[▽] Yang Li,[▽] Qi Chen, Jiaxin Liu, Kailai Yang, Meng Liang, Xiaoyan Yi, Junxi Wang, Jinmin Li, Junjie Kang,* Peng Gao,* and Zhiqiang Liu*

Cite This: *Nano Lett.* 2024, 24, 7458−7466 Read Online

ACCESS | Metrics & More | Article Recommendations | Supporting Information

ABSTRACT: The majority of dislocations in nitride epilayers are edge threading dislocations (TDs), which diminish the performance of nitride devices. However, it is extremely difficult to reduce the edge TDs due to the lack of available slip systems. Here, we systematically investigate the formation mechanism of edge TDs and find that besides originating at the coalescence boundaries, these dislocations are also closely related to geometrical misfit dislocations at the interface. Based on this understanding, we propose a novel strategy to reduce the edge TD density of the GaN epilayer by nearly 1 order of magnitude via graphene-assisted remote heteroepitaxy. The first-principles calculations confirm that the insertion of graphene dramatically reduces the energy barrier required for interfacial sliding, which promotes a new strain release channel. This work provides a unique approach to directly suppress the formation of edge TDs at the source, thereby facilitating the enhanced performance of photoelectronic and electronic devices.

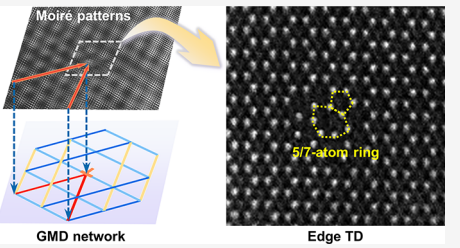

KEYWORDS: *edge threading dislocations, graphene, remote heteroepitaxy, nitride films, spontaneous strain relaxation*

Group III nitrides, including InN, GaN, and AlN are widely used in blue, green, and ultraviolet light emitting diodes (LEDs) and laser diodes,[1−3] as well as in high electron mobility transistors.[4,5] However, GaN is mostly heteroepitaxially grown on a sapphire substrate due to the large lattice and thermal mismatches between GaN and sapphire,[6] resulting in large biaxial stress in nitride crystals and high threading dislocation (TD) densities of 10^8−10^{10} cm^{-2}. There is a consensus that TDs in active regions, acting as nonradiative recombination centers, could be partially responsible for the drop in internal quantum efficiency observed in deep green and red III-nitride LEDs.[7−9] In addition, TDs significantly degrade the device performance of high electron mobility transistors by acting as charged scattering centers to affect the carrier mobility.[10−13] Furthermore, TDs cause electrical shorts in Schottky devices because they provide leakage paths along their dislocation lines and result in the breakdown voltage of high-power GaN-based devices considerably below the theoretical value.[14−16] Hence, the reduction of TDs emerges as one of the pivotal factors in the attainment of high-performance nitride devices.

Unlike the cubic crystal system,[17] nitrides possess the wurtzite structure in which the slip planes of edge TDs are prismatic $\{10\bar{1}0\}$.[18,19] In polar *c*-oriented heteroepitaxy, the prismatic planes lack resolved shear stresses. Thus, pure edge dislocations are immobile and difficult to eliminate by mutual reaction.[20−22] To make matters worse, the most possible reaction between pairs of TDs, i.e., reaction between $(\mathbf{a} + \mathbf{c})$ and $(\mathbf{a} - \mathbf{c})$, results in $\mathbf{a} + \mathbf{a}$.[23] That means this reaction does not contribute to the reduction of edge TDs and worsens the overall TD density reduction by the elimination of mobile TDs.[19] Hence, the current strategies that rely on promoting TD interactions to decrease TDs in nitride heteroepitaxy are extremely inefficient. In other words, once a TD occurs, it is extremely difficult to eliminate. Thus, it is crucial to understand the underlying origin of TDs and then suppress their formation at the source.

There is still considerable controversy regarding the origin of TDs in the nitrides. One model proposes that TDs originate at the coalescence boundaries of misoriented (i.e., tilted and twisted) islands during film growth.[24−26] Recently, Wang et al.[27] efficiently suppressed the generation of TDs during AlN column coalescence by out-of-plane and in-plane orientation control. Given the large film−substrate lattice mismatch, partial TDs could also have arisen at the mismatch interface prior to any island coalescence.[28−30] The majority of current studies omit the discussion of this part of the TDs. Though our previous work[31] has experimentally proven the suppression of such TDs by modulating the mismatch interface, the underlying mechanism and specific evolution process of these TDs have not been fully discussed. This knowledge

Received: April 11, 2024
Revised: June 5, 2024
Accepted: June 7, 2024
Published: June 11, 2024

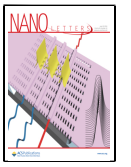

https://doi.org/10.1021/acs.nanolett.4c01724
Nano Lett. 2024, 24, 7458−7466

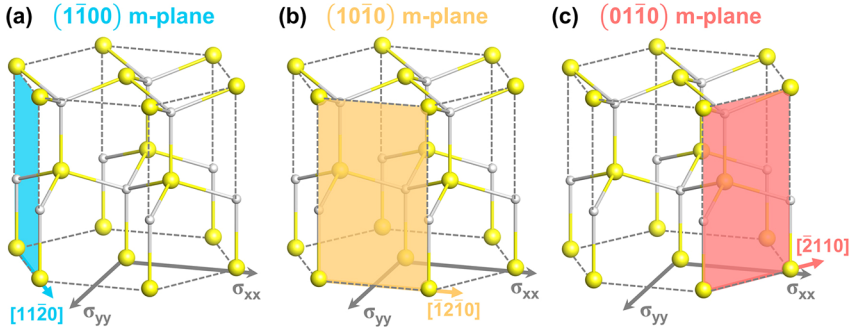

Figure 1. Three prismatic slip systems in a hexagonal wurtzite lattice. (a) (1$\bar{1}$00)[11$\bar{2}$0] (b) (10$\bar{1}$0)[$\bar{1}$2$\bar{1}$0] (c) (01$\bar{1}$0)[$\bar{2}$110]. Slip planes and directions are listed as indicated. The crystal directions of σ_{xx} and σ_{yy} are [$\bar{1}$2$\bar{1}$0] and [10$\bar{1}$0], respectively.

gap hinders the development of an effective strategy for their elimination.

In this work, we demonstrate that the occurrence of edge TDs at the interface is intensely associated with geometrical misfit dislocations (GMDs) by plane-view high-resolution transmission electron microscopy (HRTEM). Building upon this understanding, we construct a slippery interface using the graphene buffer layer, introducing a new lattice strain release mode that effectively suppresses the generation of edge TDs. Specifically, the edge TD density of a GaN film via graphene-assisted remote epitaxy is considerably reduced by nearly an order of magnitude compared to that of conventional heteroepitaxy. Furthermore, the physical mechanism of lattice strain relaxation induced by graphene is elucidated by first-principles calculations. We find that the GaN/graphene/Al_2O_3 interface substantially releases the initial in-plane strain through interface sliding, facilitated by the substantial reduction of the sliding energy barrier. Therefore, the source of edge-type dislocations, i.e., GMDs, could be effectively suppressed, eventually reducing the density of edge TDs. These results provide a novel paradigm to straightforwardly suppress TDs of III-nitride films at the heterointerface and open a new pathway for the epitaxy of high-quality nitride films.

Cubic semiconductors easily experience TD glide driven by the resolved shear stress on inclined slip planes, prompting reactions between dislocations.[19,20] However, the situation is entirely different for nitrides, which typically have a hexagonal wurtzite structure and are oriented along the [0001] direction. In nitrides, the predominant type of TD is edge dislocations, which possess the slip system of {1$\bar{1}$00}⟨11$\bar{2}$0⟩. As depicted in Figure 1a–c, the main driving force for the glide of TDs is biaxial stress, i.e., σ_{xx}, σ_{yy}, acting on the interfacial plane due to lattice mismatch. According to the Schmid law,[32] for glide to occur, the slip system should experience a resolved shear component on the slip plane and in the slip direction. For the slip system of {1$\bar{1}$00}⟨11$\bar{2}$0⟩, the calculations of the Schmid factors $\cos(\vec{b}, \vec{F})\cos(\vec{n},\vec{F})$ are presented in Table 1, where $\vec{b}$, $\vec{F}$, and $\vec{n}$ are the Burgers vector, the biaxial stress, and the normal to the gliding plane, respectively. The Schmid factors of two orientations are considered under biaxial stress with two perpendicular in-plane directions. Apparently, the algebraic sum of the Schmid factors is zero for each prismatic slip systems. Based on the analysis performed, we can conclude that these prismatic slip systems do not undergo a shear component of the lattice mismatch stress, indicating that the pure edge TDs are immobile. This implies that the interactions

Table 1. Schmid Factors Calculated for the Different Prismatic Slip Systems

	slip system	$\vec{n}$	$\vec{b}$	Schmid factors σ_{xx}[$\bar{1}$2$\bar{1}$0]	Schmid factors σ_{yy}[10$\bar{1}$0]
prismatic planes	(1$\bar{1}$00) [11$\bar{2}$0]	[1$\bar{1}$00]	[11$\bar{2}$0]	$-\sqrt{3}/4$	$\sqrt{3}/4$
	(10$\bar{1}$0) [$\bar{1}$2$\bar{1}$0]	[10$\bar{1}$0]	[$\bar{1}$2$\bar{1}$0]	0	0
	(01$\bar{1}$0) [$\bar{2}$110]	[01$\bar{1}$0]	[$\bar{2}$110]	$\sqrt{3}/4$	$-\sqrt{3}/4$

of TDs in nitrides are difficult and inefficient, which constrains a further decrease of TD density.

To comprehensively clarify the evolution of TDs at the mismatched interface and suppress the generation of TDs at the initial state of epitaxy, it is crucial to thoroughly analyze the large mismatched heterointerfaces. Thus, cross-sectional scanning transmission electron microscopy (STEM) (Figure 2a) is utilized to reveal the atomic arrangement of the GaN/Al_2O_3 heterointerface obtained via traditional heteroepitaxy. The corresponding geometric phase analysis (GPA) e_{xx} mapping image, as depicted in Figure 2b, delineates the in-plane strain distribution at the heterointerface. Periodic arrays of strain cores induced by geometrical misfit dislocations (GMDs)[33] are clearly observed at the GaN/Al_2O_3 interface. Furthermore, the fast Fourier filtered image (Figure 2c) reveals periodic arrays of dislocation cores, which are the edge component of one set of GMDs.[34,35] As shown in Figure 2c, the approximate ratio, *m*:*n*, for the {10$\bar{1}$0} planes of GaN and {11$\bar{2}$0} planes of sapphire is 7:8, indicating that one GMD should be introduced for every 7 GaN atomic planes or 8 Al_2O_3 atomic planes.[24]

For a more in-depth investigation of the GMDs at the interface, a plane-view specimen of GaN/Al_2O_3 is adequately analyzed. The Supporting Information (Figure S1) presents a plane-view HRTEM image along the [0001] axis of GaN/Al_2O_3. The Fourier filtering (Figure 2d) is performed by placing masks around the Bragg spots of Figure S1 to improve the image clarity. In Figure 2d, distinct Moiré patterns are observed, which are induced by interference of the overlapped lattice of Al_2O_3 and GaN. The appearance of Moiré patterns with a certain periodicity, known as Moiré periodicity, could also signify features of GMDs, as their periodicities are identical. Hence, the concurrent observation of Moiré pattern deformation and the termination of two GMDs is depicted in Figure 2d, with the former indicated by the white dashed ellipse and the latter by two yellow arrows. The deformation of Moiré patterns could be employed as a method to characterize

https://doi.org/10.1021/acs.nanolett.4c01724
Nano Lett. 2024, 24, 7458−7466

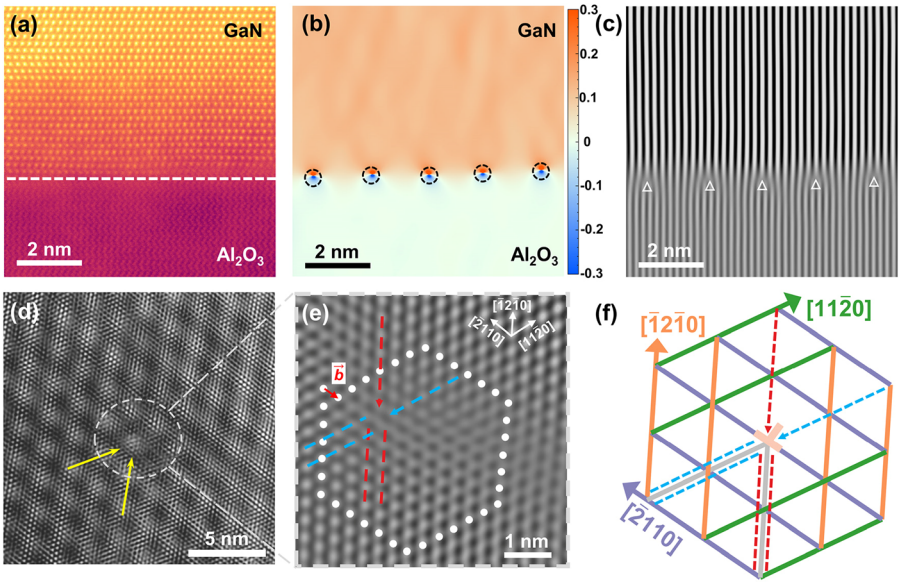

Figure 2. Evolution mechanism of edge TDs at the GaN/Al_2O_3 interface. (a) Cross-sectional STEM image of the GaN/Al_2O_3 interface, viewed along the $\langle 11\bar{2}0\rangle_{GaN}/\langle 10\bar{1}0\rangle_{Al_2O_3}$. White dashed line in (a) denotes the position of the interface. (b) GPA e_{xx} mapping images based on STEM images (panel a). The black dashed circles in panel b indicate strain cores at the interface. (c) IFFT image of the GaN/Al_2O_3 interface. The white triangles in panel c denote the position of GMDs. (d) Filtered image of Figure S1 by placing masks around the Bragg spots to improve image contrast. The white dashed ellipse depicts the deformation of Moiré patterns, and the yellow arrows indicate the termination of two GMDs. (e) IFFT image of a magnified area of panel d, masking other regions except six diffraction spots of $\{10\bar{1}0\}_{GaN}$ in order to reveal solely the GaN structure. The extra half-planes coincide with the red and blue dashed arrows pointing toward the core of the TD and the white circles indicate the Burgers circuit. (f) Schematic illustration of the fusion reaction between two GMDs. The red and blue dashed arrows represent the two additional GaN half-planes corresponding to those in panel e, and the two gray thick lines indicate the termination of GMDs.

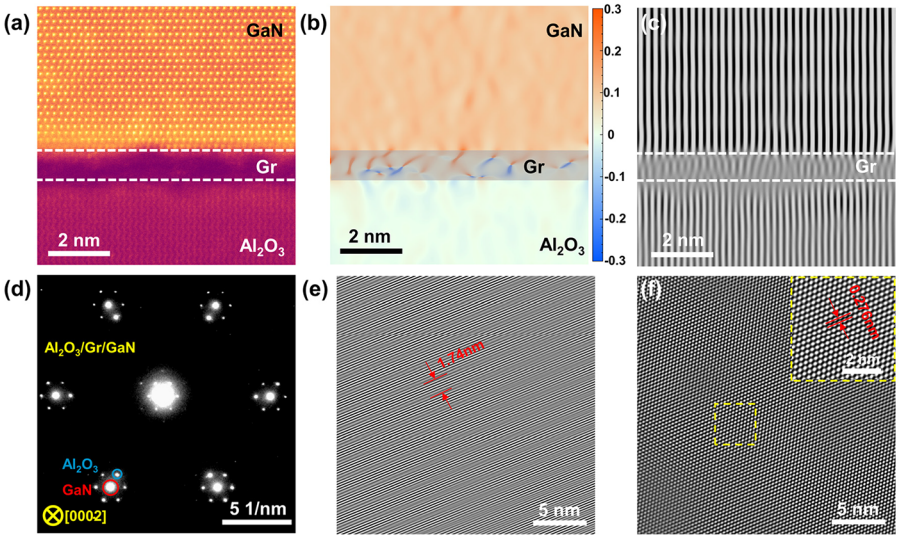

Figure 3. Cross-sectional STEM and plane-view HRTEM characterizations of the GaN/graphene (Gr)/Al_2O_3 interface. (a) Cross-sectional STEM image of the GaN/Gr/Al_2O_3 interface, viewed along the $\langle 11\bar{2}0\rangle_{GaN}/\langle 11\bar{2}0\rangle_{GaN}/\langle 10\bar{1}0\rangle_{Al_2O_3}$. White dashed lines in panel a denote the position of the interface. (b) GPA e_{xx} mapping images based on STEM images (panel a). (c) IFFT image of the GaN/Gr/Al_2O_3 interface. (d) SAED patterns of the GaN/Gr/Al_2O_3 plane-view sample. (e) One set of Moiré fringes by selecting the diffraction spots of Figure S3 corresponding to the $(1\bar{1}00)_{GaN}$ and $(1\bar{2}10)_{Al_2O_3}$ planes (f) IFFT images of Figure S3 in order to reveal solely the GaN structure.

crystal defects, which disrupt the periodicity of the interfacial lattice.[36] To identify the specific type of defect, an inverse fast Fourier transform (IFFT) image of the marked region in Figure 2d is shown in Figure 2e. The diffraction spots of $\{10\bar{1}0\}_{GaN}$ are selected for revealing solely the GaN atomic structure. Notably, the crystal defect is intimately associated with the presence of two additional $\{10\bar{1}0\}_{GaN}$ half-planes, identified by the red and blue dashed arrows in Figure 2e. To more reliably determine the atomic structure of this defect, depth-sectioning high-angle annular dark-field (HAADF) STEM[37,38] is performed in the marked region of Figure 2d. By focusing on the top surface of the GaN epilayer, the defect is identified as a 5/7-atom ring structure, as illustrated in Figure S2a. It is widely known that the core of pure edge TDs in GaN is a 5/7-atom ring structure,[39,40] characterized by the insertion of two extra $\{10\bar{1}0\}_{GaN}$, as shown in Figure S2b.

https://doi.org/10.1021/acs.nanolett.4c01724
Nano Lett. 2024, 24, 7458−7466

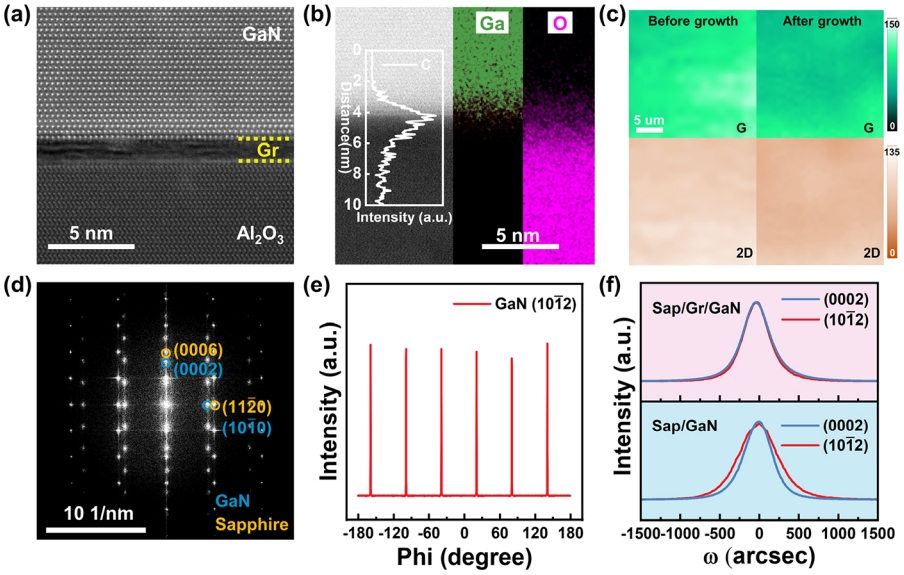

Figure 4. Characterization of the single crystalline GaN film grown on the Gr/sapphire substrate. (a) Cross-sectional STEM image of the GaN/Gr/Al_2O_3 interface, layers from bottom to top are Al_2O_3, graphene, and GaN, respectively. (b) EDS linear scanning spectrum of C element and EDS mappings of Ga (green) and O (purple) elements at the interface (c) Raman mapping of G and 2D peaks of Gr in a 25 × 25 μm^2 before and after growth of GaN by MOCVD. (d) Electron diffraction patterns from the interface of GaN/Gr/sapphire. The blue and orange circles indicate the patterns from GaN and sapphire, respectively. (e) XRD ϕ-scan of the GaN epilayer (10$\bar{1}$2) planes. (f) X-ray rocking curve of (0002) and (10$\bar{1}$2) for GaN epilayers grown on sapphire with (above) and without (bottom) Gr.

Consequently, this defect responsible for the deformation of Moiré patterns could be an edge TD. This conclusion is further supported by determining the Burgers vector to be 1/3⟨11$\bar{2}$0⟩ indicated by the white loop in Figure 2e. Considering the Burgers vectors of both the TD (**b** = $\mathbf{a}_1$) and two GMDs (**b** = $\mathbf{a}_2$, $\mathbf{a}_3$),[34] it is found that these two extra prismatic half-planes produce the edge TD, while simultaneously annihilating two GMDs, by a fusion reaction $\mathbf{a}_1 = \mathbf{a}_2 + \mathbf{a}_3$. The fusion reaction between two GMDs is also schematically shown in Figure 2f. Considering that the energy of dislocations is proportional to b^2,[41] such a fusion reaction is energetically favorable. Hence, this could spontaneously occur and lead to the formation of edge TDs at the interface. In short, for the traditional heteroepitaxy of large-mismatch systems, GMDs are primarily responsible for releasing the mismatch strain. However, they concurrently serve as a source for forming edge TDs at the interface, thereby impeding the efficient reduction of the TD density in nitrides.

These analyses lead to reasonable speculation that the highly effective reduction of edge TDs lies in the reconstruction of a heterointerface, aiming at modulating the mismatch strain and suppressing the generation of GMDs. Recently, the growth of the nitrides via graphene-assisted remote epitaxy[42−52] has been implemented, successfully constructing a slippery interface for strain release.[53−61] Especially, crystallographic defects in heteroepitaxial layers could be substantially reduced with the assistance of nanopatterned graphene.[62,63] Hence, graphene is chosen as an interlayer to facilitate the reconstruction of the heterointerface. The cross-sectional STEM of the GaN/Gr/Al_2O_3 interface and corresponding GPA e_{xx} mapping image are shown in Figure 3a,b, respectively. Strain cores induced by GMDs with the typical tension−compression contrast are not observed at the interface with graphene. Moreover, the fast Fourier filtered image (Figure 3c) also illustrates that the insertion of graphene significantly reduces the periodic edge dislocation cores at the interface, with only distorted and blurred pseudolattice fringes attributed to phase errors being observed at the location of graphene. The selected area electron diffraction (SAED) pattern along the [0001] direction of the GaN/graphene/Al_2O_3 plane sample is presented in Figure 3d, where satellite spots appear around the basic reflection of the GaN crystal due to double diffraction. Figure 3e shows the IFFT image of Figure S3 by selecting the diffraction spots corresponding to the $(1\bar{1}00)_{GaN}$ and $(1\bar{2}10)_{Al_2O_3}$ planes. The highly periodic Moiré fringes demonstrate that the insertion of graphene significantly suppresses the local distortions, i.e., edge TDs at the interface. And the measured spacing of the Moiré fringes is 1.74 nm, indicating that the GaN epitaxial layer is under slight compressive stress (see the Supporting Information for the more detailed calculation). Additionally, the stress of the GaN film was quantitatively investigated by Raman measurements (Figure S4). In comparison to Figure 2e, a more ordered atomic arrangement of GaN is revealed (Figure 3f) and the *d*-spacing of $\{10\bar{1}0\}_{GaN}$ is measured as 0.276 nm (inset of Figure 3f). In two-beam conditions, Moiré fringes generated by the (01$\bar{1}$0) plane of GaN and the ($\bar{1}$2$\bar{1}$0) plane of Al_2O_3 are observed in the absence (Figure S5c) and presence (Figure S5d) of graphene. Through the calculation of the terminations of Moiré fringes, the dislocation densities are measured separately from the various areas of Moiré fringes, roughly at the order of 3.9 × 10^{12} cm^{-2} (without graphene) and 4.4 × 10^{11} cm^{-2} (with graphene), respectively. The enhancement of the near-band-edge photoluminescence intensity also demonstrates the superior crystal quality of the GaN grown on the Gr/Al_2O_3 substrate (Figure S7).

Furthermore, the crystalline quality of GaN on the graphene-coated sapphire substrate was thoroughly characterized. Figure 4a shows an atomically resolved STEM image of the GaN/graphene/Al_2O_3 interface, where the presence of graphene is clearly distinguished at the interface. Simultaneously, the corresponding energy dispersive X-ray spectros-

https://doi.org/10.1021/acs.nanolett.4c01724
Nano Lett. 2024, 24, 7458−7466

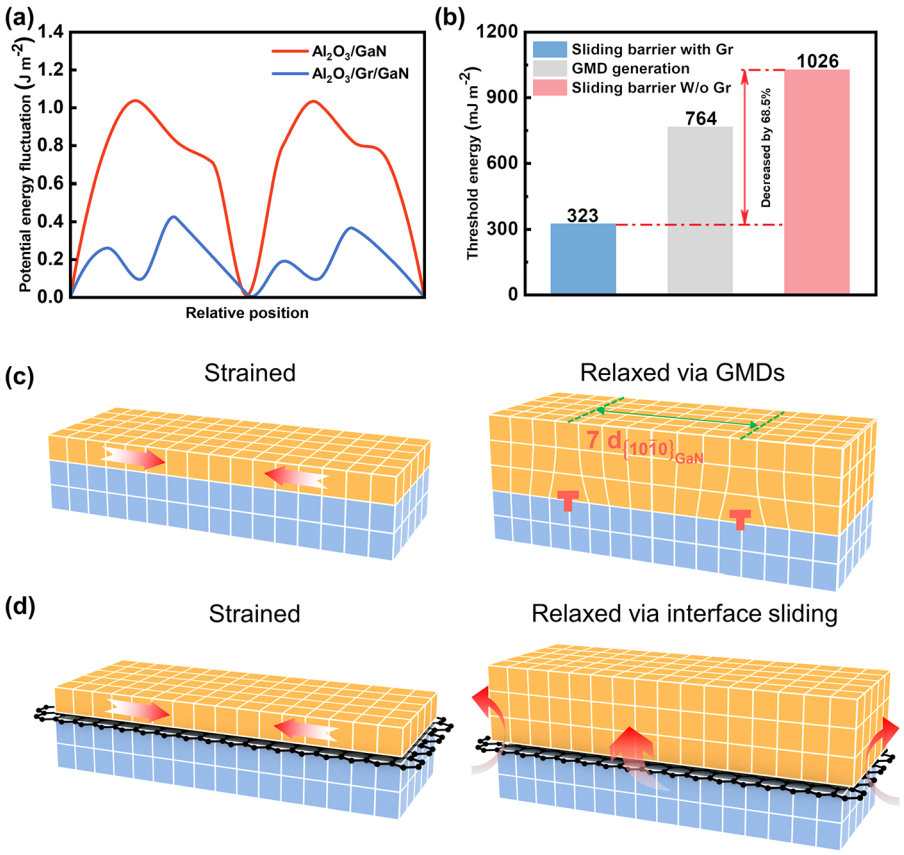

Figure 5. Theoretical calculations and mechanisms of strain alleviation at the heterointerface. (a) Energy barrier required for the interface sliding of GaN/Al_2O_3 and GaN/Gr/Al_2O_3. (b) Threshold energy for the situations of interface sliding on graphene (323 mJ m^{-2}), the introduction of a GMD (764 mJ m^{-2}), and interface sliding on bare sapphire (1026 mJ m^{-2}). (c) Schematic diagram of strain relaxation via the introduction of the periodic geometrical misfit dislocation network. (d) Schematic diagram of strain relaxation via interface sliding.

copy (EDS) linear scanning of the C element and EDS mapping of Ga and O elements (Figure 4b) also confirm the existence of graphene. The intact preservation of graphene after metal−organic chemical vapor deposition (MOCVD) growth is confirmed by Raman mapping (Figure 4c). The intensity ratio of the 2D peak to G peak is ∼0.92, indicating the ∼2 layer feature of the graphene.[64] Subsequent to nitride growth, a discernible decrease in the value of I_{2D}/I_G accompanied by a broadened and more pronounced D peak indicates the formation of defects during the process of growth (Figure S9).[65] The alignment of diffraction spots in the electron diffraction patterns from the interface (Figure 4d) indicates that the epitaxial relationship between GaN and sapphire is defined as $(0001)_{GaN}\|(0001)_{sapphire}$, $[10\bar{1}0]_{GaN}\|[11\bar{2}0]_{sapphire}$. This configuration demonstrates a 30° twisted angle between the epilayer and sapphire through graphene, which is consistent with the observed outcome of GaN growth directly on a bare sapphire substrate.[66] The X-ray diffraction (XRD) ϕ-scan (Figure 4e) shows one set of peaks with a 60° period, possessing 6-fold symmetry of the GaN single crystal. In particular, the fwhm of (0002) and (10$\bar{1}$2) peaks (Figure 4f) of GaN film with graphene are 408 arcsec and 386 arcsec, respectively, corresponding to 3.35×10^8 cm^{-2} and 6.83×10^8 cm^{-2} densities of screw and edge dislocations. In contrast, the fwhm of (0002) and (10$\bar{1}$2) peaks of GaN without graphene are 416 arcsec and 586 arcsec, corresponding to 3.48×10^8 cm^{-2} and 2.85×10^9 cm^{-2} densities of screw and edge dislocations,[67] respectively. Therefore, in the case of graphene-assisted remote epitaxy, our findings reveal that the fwhm of the (10$\bar{1}$2) peak is even smaller than that of (0002), and the edge TD density is reduced by nearly an order of magnitude compared to the conventional heteroepitaxy.

To further understand the underlying mechanism of strain relaxation induced by graphene, we conducted first-principles calculations. As shown in Figure 5a, density functional theory (DFT) calculations reveal a significantly reduced energy barrier required for interface displacement on a graphene surface compared to that on a bare sapphire substrate (see Supporting Information for comprehensive details of DFT calculation). Thus, our calculations demonstrate that the insertion of graphene considerably increases the possibility of interface displacement, in agreement with previous reports.[53,57] In addition, the strain release process at the heterointerface could be speculated by elastic energy analysis. The maximum energy barrier for the GaN epilayer displacement on graphene-coated sapphire is calculated to be 323 mJ m^{-2}, while the calculated elastic energy required for the introduction of a GMD is 764 mJ m^{-2} by using dislocation theory (see the Supporting Information for details).[22] In contrast, the energy required for displacing the GaN epilayer directly on a bare sapphire substrate is 1026 mJ m^{-2}, as depicted in Figure 5b. Accordingly, considering the reduced interfacial potential barrier for interfacial sliding, the graphene-based remote epitaxy system appears to be more favorable for alleviating the large mismatch strain at the interface by spontaneous

https://doi.org/10.1021/acs.nanolett.4c01724
Nano Lett. 2024, 24, 7458−7466

lattice relaxation rather than by the formation of GMDs in traditional heteroepitaxy.

With the above discussion and analysis, the mechanism of remote epitaxy in large mismatched systems to reduce the density of edge TDs is schematically exhibited in Figure 5c,d. Specifically, due to the robust covalent bond formation between the GaN epilayer and the rigid sapphire substrate, the initial relaxation in the highly mismatched heteroepitaxial system could only occur via the establishment of a geometrical misfit dislocation network, facilitating the near coincident site lattice at the interface. Nonetheless, once GaN epitaxy is performed on a graphene-coated sapphire substrate, the binding energy between the epitaxial layer and the substrate is weakened, allowing the spontaneous relaxation of the misfit strain by interfacial displacement (Figure 5d). As a result, spontaneous lattice relaxation of the GaN films effectively accommodates the substantial mismatch at the interface, thereby reducing the formation of GMDs. In essence, our demonstration underscores that the interaction among GMDs stands as a fundamental factor contributing to the formation of edge TDs. The insertion of graphene leads to a remarkable reduction in GMD generation, which efficiently decreases the density of edge TDs.

In summary, we clarified the intense association between edge TDs and GMDs at the interface using HRTEM in a plane-view geometry. According to this analysis, we propose a novel approach to directly suppress the formation of edge TDs in III-nitride epitaxy through constructing the GaN/graphene/Al_2O_3 interface. The insertion of a graphene layer establishes a slippery interface, introducing a new pathway for lattice strain release. Notably, the density of edge-type dislocations in the obtained nitride films is reduced by nearly an order of magnitude compared with that of the conventional heteroepitaxy. Additionally, a physical model is introduced to elucidate the mechanism of strain relaxation induced by graphene. The interfacial slip potential barrier of the GaN/graphene/Al_2O_3 interface substantially decreases compared to that of the GaN/Al_2O_3 interface by the first-principles calculations. Consequently, the graphene-based remote epitaxy systems exhibit a preference for spontaneous lattice relaxation over the formation of GMDs, when releasing the large mismatch strain. And given the strong correlation of edge TDs and GMDs, the generation of edge TDs is effectively suppressed. This work sheds light on the direct suppression of TDs at the heterointerface and paves the way for epitaxy of high-quality III-nitride films on large lattice mismatched foreign substrates, promising advancements in the fabrication of advanced photoelectronic and electronic devices.

■ ASSOCIATED CONTENT

Supporting Information

The Supporting Information is available free of charge at https://pubs.acs.org/doi/10.1021/acs.nanolett.4c01724.

HRTEM images of the GaN/Al_2O_3 plane-view sample; The atomic core structure of edge threading dislocation; HRTEM images of the GaN/Gr/Al_2O_3 plane-view sample; Raman spectra of GaN epilayers with and without Gr; Moiré fringes in HRTEM BF plane-view images of the plane samples; electron diffraction patterns in both plane-view and cross-section; PL spectra of GaN epilayers with and without Gr; surface morphology of the GaN film grown on Gr/sapphire substrate; Raman spectra of graphene; geometrical phase analysis for strain mapping; calculation of the compressive strain relaxation through the interface sliding; computational details of the calculation of energy barrier for surface sliding; calculation details of the energy density of geometrical misfit dislocation (PDF)

■ AUTHOR INFORMATION

Corresponding Authors

Junjie Kang − *Research and Development Center for Solid State Lighting, Institute of Semiconductors, Chinese Academy of Sciences, Beijing 100083, China; Center of Materials Science and Optoelectronics Engineering, University of Chinese Academy of Sciences, Beijing 100049, China*; Email: kangjunjie@semi.ac.cn

Peng Gao − *Electron Microscopy Laboratory, and International Center for Quantum Materials, School of Physics, Peking University, Beijing 100871, China*; orcid.org/0000-0003-0860-5525; Email: p-gao@pku.edu.cn

Zhiqiang Liu − *Research and Development Center for Solid State Lighting, Institute of Semiconductors, Chinese Academy of Sciences, Beijing 100083, China; Center of Materials Science and Optoelectronics Engineering, University of Chinese Academy of Sciences, Beijing 100049, China*; orcid.org/0000-0002-5341-0463; Email: lzq@semi.ac.cn

Authors

Bo Shi − *Research and Development Center for Solid State Lighting, Institute of Semiconductors, Chinese Academy of Sciences, Beijing 100083, China; Center of Materials Science and Optoelectronics Engineering, University of Chinese Academy of Sciences, Beijing 100049, China*

Zhetong Liu − *Electron Microscopy Laboratory, and International Center for Quantum Materials, School of Physics, Peking University, Beijing 100871, China*

Yang Li − *Research and Development Center for Solid State Lighting, Institute of Semiconductors, Chinese Academy of Sciences, Beijing 100083, China; Center of Materials Science and Optoelectronics Engineering, University of Chinese Academy of Sciences, Beijing 100049, China*

Qi Chen − *Research and Development Center for Solid State Lighting, Institute of Semiconductors, Chinese Academy of Sciences, Beijing 100083, China; Center of Materials Science and Optoelectronics Engineering, University of Chinese Academy of Sciences, Beijing 100049, China*

Jiaxin Liu − *Electron Microscopy Laboratory, and International Center for Quantum Materials, School of Physics, Peking University, Beijing 100871, China*

Kailai Yang − *Research and Development Center for Solid State Lighting, Institute of Semiconductors, Chinese Academy of Sciences, Beijing 100083, China; Center of Materials Science and Optoelectronics Engineering, University of Chinese Academy of Sciences, Beijing 100049, China*

Meng Liang − *Research and Development Center for Solid State Lighting, Institute of Semiconductors, Chinese Academy of Sciences, Beijing 100083, China; Center of Materials Science and Optoelectronics Engineering, University of Chinese Academy of Sciences, Beijing 100049, China*

Xiaoyan Yi − *Research and Development Center for Solid State Lighting, Institute of Semiconductors, Chinese Academy of Sciences, Beijing 100083, China; Center of Materials Science*

https://doi.org/10.1021/acs.nanolett.4c01724
Nano Lett. 2024, 24, 7458−7466

and Optoelectronics Engineering, University of Chinese Academy of Sciences, Beijing 100049, China

Junxi Wang − *Research and Development Center for Solid State Lighting, Institute of Semiconductors, Chinese Academy of Sciences, Beijing 100083, China; Center of Materials Science and Optoelectronics Engineering, University of Chinese Academy of Sciences, Beijing 100049, China;* orcid.org/0000-0002-8283-5540

Jinmin Li − *Research and Development Center for Solid State Lighting, Institute of Semiconductors, Chinese Academy of Sciences, Beijing 100083, China; Center of Materials Science and Optoelectronics Engineering, University of Chinese Academy of Sciences, Beijing 100049, China*

Complete contact information is available at: https://pubs.acs.org/10.1021/acs.nanolett.4c01724

Author Contributions

[∇]B. S., Z. T. L., and Y. L. contributed equally to this work. J. J. K, P. G., and Z. Q. L. conceived the idea and designed this work. B. S, Z. T. L., M. L., and Q. C. conceived the experiment. Z. T. L. and J. X. L. carried out the TEM characterization. B. S., Y. L., and Q. C. contributed to the data summary and figure configuration. B. S. and K. L. Y. carried out the first-principles calculations. All authors discussed the results and commented on the manuscript.

Notes

The authors declare no competing financial interest.

■ ACKNOWLEDGMENTS

The work was supported by the National Key Research and Development Program of China (Grant Nos. 2021YFB3600400, 2019YFA0708200, 2023YFB3611200 and 2023YFB3609900), the National Natural Science Foundation of China (Grant No. 62174157).

■ REFERENCES

(1) Wasisto, H. S.; Prades, J. D.; Gulink, J.; Waag, A. Beyond solid-state lighting: Miniaturization, hybrid integration, and applications of GaN nano-and micro-LEDs. *Appl. Phys. Rev.* **2019**, *6* (4), 041315.

(2) Ponce, F. A.; Bour, D. P. Nitride-based semiconductors for blue and green light-emitting devices. *Nature* **1997**, *386* (6623), 351−359.

(3) Templier, F. GaN-based emissive microdisplays: a very promising technology for compact, ultra-high brightness display systems. *J. Soc. Inf. Dispersion* **2016**, *24* (11), 669−675.

(4) Baliga, B. J. Gallium nitride devices for power electronic applications. *Semicond. Sci. Technol.* **2013**, *28* (7), 074011.

(5) Jones, E. A.; Wang, F. F.; Costinett, D. Review of commercial GaN power devices and GaN-based converter design challenges. *IEEE Trans. Emerg. Sel. Topics Power Electron.* **2016**, *4* (3), 707−719.

(6) Zhao, D. G.; Xu, S. J.; Xie, M. H.; Tong, S. Y.; Yang, H. Stress and its effect on optical properties of GaN epilayers grown on Si (111), 6H-SiC (0001), and c-plane sapphire. *Appl. Phys. Lett.* **2003**, *83* (4), 677−679.

(7) Nakamura, S. The roles of structural imperfections in InGaN-based blue light-emitting diodes and laser diodes. *Science* **1998**, *281* (5379), 956−961.

(8) Reshchikov, M. A.; Morkoc, H. Luminescence properties of defects in GaN. *J. Appl. Phys.* **2005**, *97* (6), 5−19.

(9) Khan, A.; Balakrishnan, K.; Katona, T. Ultraviolet light-emitting diodes based on group three nitrides. *Nat. Photonics* **2008**, *2* (2), 77−84.

(10) Hino, T.; Tomiya, S.; Miyajima, T.; Yanashima, K.; Hashimoto, S.; Ikeda, M. Characterization of threading dislocations in GaN epitaxial layers. *Appl. Phys. Lett.* **2000**, *76* (23), 3421−3423.

(11) Weimann, N. G.; Eastman, L. F.; Doppalapudi, D.; Ng, H. M.; Moustakas, T. D. Scattering of electrons at threading dislocations in GaN. *J. Appl. Phys.* **1998**, *83* (7), 3656−3659.

(12) Look, D. C.; Sizelove, J. R. Dislocation Scattering in GaN. *Phys. Rev. Lett.* **1999**, *82*, 1237−1240.

(13) Morkoc, B. H.; Strite, S.; Gao, G. B.; Lin, M. E.; Sverdlov, B.; Burns, M. Large-band-gap SiC, III-V nitride, and II-VI ZnSe-based semiconductor device technologies. *J. Appl. Phys.* **1994**, *76* (3), 1363−1398.

(14) Hsu, J. W. P.; Manfra, M. J.; Molnar, R. J.; Heying, B.; Speck, J. S. Direct imaging of reverse-bias leakage through pure screw dislocations in GaN films grown by molecular beam epitaxy on GaN templates. *Appl. Phys. Lett.* **2002**, *81* (1), 79−81.

(15) Wang, J.; You, H.; Guo, H.; Xue, J.; Yang, G.; Chen, D.; Liu, B.; Lu, H.; Zhang, R.; Zheng, Y. Do all screw dislocations cause leakage in GaN-based devices? *Appl. Phys. Lett.* **2020**, *116* (6), 062104.

(16) Dickerson, J. R.; Allerman, A. A.; Bryant, B. N.; Fischer, A. J.; King, M. P.; Moseley, M. W.; Armstrong, A. M.; Kaplar, R. J.; Kizilyalli, I. C.; Aktas, O.; Wierer, J. J. Vertical GaN power diodes with a bilayer edge termination. *IEEE Trans. Electron Devices* **2016**, *63* (1), 419−425.

(17) Sheldon, P.; Jones, K. M.; Al-Jassim, M. M.; Yacobi, B. G. Dislocation density reduction through annihilation in lattice-mismatched semiconductors grown by molecular-beam epitaxy. *J. Appl. Phys.* **1988**, *63* (11), 5609−5611.

(18) Srinivasan, S.; Geng, L.; Liu, R.; Ponce, F.; Narukawa, Y.; Tanaka, S. Slip systems and misfit dislocations in InGaN epilayers. *Appl. Phys. Lett.* **2003**, *83* (25), 5187−5189.

(19) Ward, T.; Sanchez, A. M.; Tang, M.; Wu, J.; Liu, H.; Dunstan, D. J.; Beanland, R. Design rules for dislocation filters. *J. Appl. Phys.* **2014**, *116* (6), 063508.

(20) Hawkridge, M.; Cherns, D.; Myers, T. Lateral migration of dislocations in oxygen-doped GaN grown by molecular beam epitaxy. *Appl. Phys. Lett.* **2006**, *89* (25), 251915.

(21) Yakimov, E. B.; Vergeles, P. S.; Polyakov, A. Y.; Lee, I.-H.; Pearton, S. J. Movement of basal plane dislocations in GaN during electron beam irradiation. *Appl. Phys. Lett.* **2015**, *106* (13), 132101.

(22) Lebedev, V.; Cimalla, V.; Pezoldt, J.; Himmerlich, M.; Krischok, S.; Schaefer, J. A.; Ambacher, O.; Morales, F. M.; Lozano, J. G.; Gonzalez, D. Effect of dislocations on electrical and electron transport properties of InN thin films. I. Strain relief and formation of a dislocation network. *J. Appl. Phys.* **2006**, *100* (9), 094902.

(23) Mathis, S. K.; Romanov, A. E.; Chen, L. F.; Beltz, G. E.; Pompe, W.; Speck, J. S. Modeling of threading dislocation reduction in growing GaN layers. *J. Cryst. Growth* **2001**, *231* (3), 371−390.

(24) Ning, X. J.; Chien, F. R.; Pirouz, P.; Yang, J. W.; Khan, M. A. Growth defects in GaN films on sapphire: The probable origin of threading dislocations. *J. Mater. Res. Technol.* **1996**, *11* (3), 580−592.

(25) Wu, X.; Fini, P.; Tarsa, E.; Heying, B.; Keller, S.; Mishra, U.; DenBaars, S.; Speck, J. Dislocation generation in GaN heteroepitaxy. *J. Cryst. Growth* **1998**, *189*, 231−243.

(26) Ponce, F. A. Defects and interfaces in GaN epitaxy. *MRS Bull.* **1997**, *22* (2), 51−57.

(27) Wang, J.; Xie, N.; Xu, F.; Zhang, L.; Lang, J.; Kang, X.; Qin, Z.; Yang, X.; Tang, N.; Wang, X.; et al. Group-III nitride heteroepitaxial films approaching bulk-class quality. *Nat. Mater.* **2023**, *22*, 853.

(28) Narayanan, V.; Lorenz, K.; Kim, W.; Mahajan, S. Origins of threading dislocations in GaN epitaxial layers grown on sapphire by metalorganic chemical vapor deposition. *Appl. Phys. Lett.* **2001**, *78* (11), 1544−1546.

(29) Oliver, R. A.; Kappers, M. J.; Humphreys, C. J. Insights into the origin of threading dislocations in GaN/Al_2O_3 from atomic force microscopy. *Appl. Phys. Lett.* **2006**, *89* (1), 011914.

(30) Moram, M.; Ghedia, C.; Rao, D.; Barnard, J.; Zhang, Y.; Kappers, M.; Humphreys, C. On the origin of threading dislocations in GaN films. *J. Appl. Phys.* **2009**, *106* (7), 073513.

(31) Chang, H.; Liu, Z.; Yang, S.; Gao, Y.; Shan, J.; Liu, B.; Sun, J.; Chen, Z.; Yan, J.; Liu, Z.; et al. Graphene-driving strain engineering to

enable strain-free epitaxy of AlN film for deep ultraviolet light-emitting diode. *Light Sci. Appl.* **2022**, *11* (1), 88.
(32) Fitzgerald, E. Dislocations in strained-layer epitaxy: theory, experiment, and applications. *Mater. Sci. Rep.* **1991**, *7* (3), 87−142.
(33) Ikuhara, Y.; Pirouz, P.; Heuer, A.; Yadavalli, S.; Flynn, C. Structure of V-Al2, O3 interfaces grown by molecular beam epitaxy. *Philos. Mag (Abingdon)* **1994**, *70* (1), 75−97.
(34) Ruterana, P.; Potin, V.; Barbaray, B.; Nouet, G. Growth defects in GaN layers on top of (0001) sapphire: A geometrical investigation of the misfit effect. *Philos. Mag (Abingdon)* **2000**, *80* (4), 937−954.
(35) Kehagias, T.; Komninou, P.; Nouet, G.; Ruterana, P.; Karakostas, T. Misfit relaxation of the AlN/Al_2O_3 (0001) interface. *Phys. Rev. B* **2001**, *64* (19), 195329.
(36) Mante, N.; Rennesson, S.; Frayssinet, E.; Largeau, L.; Semond, F.; Rouviere, J. L.; Feuillet, G.; Vennegues, P. Proposition of a model elucidating the AlN-on-Si (111) microstructure. *J. Appl. Phys.* **2018**, *123* (21), 215701.
(37) Sánchez-Santolino, G.; Rouco, V.; Puebla, S.; Aramberri, H.; Zamora, V.; Cabero, M.; Cuellar, F.; Munuera, C.; Mompean, F.; Garcia-Hernandez, M.; et al. A 2D ferroelectric vortex pattern in twisted BaTiO3 freestanding layers. *Nature* **2024**, *626* (7999), 529−534.
(38) Ishikawa, R.; Lupini, A. R.; Hinuma, Y.; Pennycook, S. J. Large-angle illumination STEM: toward three-dimensional atom-by-atom imaging. *Ultramicroscopy* **2015**, *151*, 122−129.
(39) Rhode, S.; Horton, M.; Kappers, M.; Zhang, S.; Humphreys, C.; Dusane, R.; Sahonta, S.-L.; Moram, M. Mg doping affects dislocation core structures in GaN. *Phys. Rev. Lett.* **2013**, *111* (2), 025502.
(40) Lymperakis, L.; Neugebauer, J.; Albrecht, M.; Remmele, T.; Strunk, H. Strain induced deep electronic states around threading dislocations in GaN. *Phys. Rev. Lett.* **2004**, *93* (19), 196401.
(41) Speck, J.; Brewer, M.; Beltz, G.; Romanov, A.; Pompe, W. Scaling laws for the reduction of threading dislocation densities in homogeneous buffer layers. *J. Appl. Phys.* **1996**, *80* (7), 3808−3816.
(42) Chen, Z.; Zhang, X.; Dou, Z.; Wei, T.; Liu, Z.; Qi, Y.; Ci, H.; Wang, Y.; Li, Y.; Chang, H.; et al. High-brightness blue light-emitting diodes enabled by a directly grown graphene buffer layer. *Adv. Mater.* **2018**, *30* (30), 1801608.
(43) Choi, J.-K.; Huh, J.-H.; Kim, S.-D.; Moon, D.; Yoon, D.; Joo, K.; Kwak, J.; Chu, J. H.; Kim, S. Y.; Park, K.; et al. One-step graphene coating of heteroepitaxial GaN films. *Nanotechnology* **2012**, *23* (43), 435603.
(44) Zhang, S.; Liu, B.; Ren, F.; Yin, Y.; Wang, Y.; Chen, Z.; Jiang, B.; Liu, B.; Liu, Z.; Sun, J.; et al. Graphene-Nanorod Enhanced Quasi-Van Der Waals Epitaxy for High Indium Composition Nitride Films. *Small* **2021**, *17* (19), 2100098.
(45) Qiao, K.; Liu, Y.; Kim, C.; Molnar, R. J.; Osadchy, T.; Li, W.; Sun, X.; Li, H.; Myers-Ward, R. L.; Lee, D.; et al. Graphene buffer layer on SiC as a release layer for high-quality freestanding semiconductor membranes. *Nano Lett.* **2021**, *21* (9), 4013−4020.
(46) Wang, Y.; Yang, S.; Chang, H.; Li, W.; Chen, X.; Hou, R.; Yan, J.; Yi, X.; Wang, J.; Wei, T. Flexible graphene-assisted van der Waals epitaxy growth of crack-free AlN epilayer on SiC by lattice engineering. *Appl. Surf. Sci.* **2020**, *520*, 146358.
(47) Feng, Y.; Yang, X.; Zhang, Z.; Kang, D.; Zhang, J.; Liu, K.; Li, X.; Shen, J.; Liu, F.; Wang, T.; et al. GaN-on-Si(100): Epitaxy of single-crystalline GaN film on CMOS-compatible Si(100) substrate buffered by graphene. *Adv. Funct. Mater.* **2019**, *29* (42), 1905056.
(48) Chung, K.; Lee, C.-H.; Yi, G.-C. Transferable GaN layers grown on ZnO-coated graphene layers for optoelectronic devices. *Science* **2010**, *330* (6004), 655−657.
(49) Lee, C. H.; Kim, Y. J.; Hong, Y. J.; Jeon, S. R.; Bae, S.; Hong, B. H.; Yi, G. C. Flexible inorganic nanostructure light-emitting diodes fabricated on graphene films. *Adv. Mater.* **2011**, *23* (40), 4614−4619.
(50) Chung, K.; Yoo, H.; Hyun, J. K.; Oh, H.; Tchoe, Y.; Lee, K.; Baek, H.; Kim, M.; Yi, G. C. Flexible GaN light-emitting diodes using GaN microdisks epitaxial laterally overgrown on graphene dots. *Adv. Mater.* **2016**, *28* (35), 7688−7694.
(51) Liu, F.; Zhang, Z.; Rong, X.; Yu, Y.; Wang, T.; Sheng, B.; Wei, J.; Zhou, S.; Yang, X.; Xu, F.; et al. Graphene-Assisted Epitaxy of Nitrogen Lattice Polarity GaN Films on Non-Polar Sapphire Substrates for Green Light Emitting Diodes. *Adv. Funct. Mater.* **2020**, *30* (22), 2001283.
(52) Jeong, J.; Wang, Q.; Cha, J.; Jin, D. K.; Shin, D. H.; Kwon, S.; Kang, B. K.; Jang, J. H.; Yang, W. S.; Choi, Y. S.; et al. Remote heteroepitaxy of GaN microrod heterostructures for deformable light-emitting diodes and wafer recycle. *Sci. Adv.* **2020**, *6* (23), No. eaaz5180.
(53) Bae, S.-H.; Lu, K.; Han, Y.; Kim, S.; Qiao, K.; Choi, C.; Nie, Y.; Kim, H.; Kum, H. S.; Chen, P. Graphene-assisted spontaneous relaxation towards dislocation-free heteroepitaxy. *Nat. Nanotechnol.* **2020**, *15* (4), 272−276.
(54) Heilmann, M.; Munshi, A. M.; Sarau, G.; Göbelt, M.; Tessarek, C.; Fauske, V. T.; van Helvoort, A. T.; Yang, J.; Latzel, M.; Hoffmann, B. r.; et al. Vertically oriented growth of GaN nanorods on Si using graphene as an atomically thin buffer layer. *Nano Lett.* **2016**, *16* (6), 3524−3532.
(55) Kum, H. S.; Lee, H.; Kim, S.; Lindemann, S.; Kong, W.; Qiao, K.; Chen, P.; Irwin, J.; Lee, J. H.; Xie, S.; et al. Heterogeneous integration of single-crystalline complex-oxide membranes. *Nature* **2020**, *578* (7793), 75−81.
(56) Kim, J.; Bayram, C.; Park, H.; Cheng, C.-W.; Dimitrakopoulos, C.; Ott, J. A.; Reuter, K. B.; Bedell, S. W.; Sadana, D. K. Principle of direct van der Waals epitaxy of single-crystalline films on epitaxial graphene. *Nat. Commun.* **2014**, *5* (1), 4836.
(57) Liu, B.; Chen, Q.; Chen, Z.; Yang, S.; Shan, J.; Liu, Z.; Yin, Y.; Ren, F.; Zhang, S.; Wang, R.; et al. Atomic Mechanism of Strain Alleviation and Dislocation Reduction in Highly Mismatched Remote Heteroepitaxy Using a Graphene Interlayer. *Nano Lett.* **2022**, *22* (8), 3364−3371.
(58) Kong, W.; Li, H.; Qiao, K.; Kim, Y.; Lee, K.; Nie, Y.; Lee, D.; Osadchy, T.; Molnar, R. J.; Gaskill, D. K.; et al. Polarity governs atomic interaction through two-dimensional materials. *Nat. Mater.* **2018**, *17* (11), 999−1004.
(59) Kum, H.; Lee, D.; Kong, W.; Kim, H.; Park, Y.; Kim, Y.; Baek, Y.; Bae, S.-H.; Lee, K.; Kim, J. Epitaxial growth and layer-transfer techniques for heterogeneous integration of materials for electronic and photonic devices. *Nat. Electron.* **2019**, *2* (10), 439−450.
(60) Liu, Y.; Huang, Y.; Duan, X. Van der Waals integration before and beyond two-dimensional materials. *Nature* **2019**, *567* (7748), 323−333.
(61) Kim, Y.; Cruz, S. S.; Lee, K.; Alawode, B. O.; Choi, C.; Song, Y.; Johnson, J. M.; Heidelberger, C.; Kong, W.; Choi, S.; et al. Remote epitaxy through graphene enables two-dimensional material-based layer transfer. *Nature* **2017**, *544* (7650), 340−343.
(62) Kim, H.; Lee, S.; Shin, J.; Zhu, M.; Akl, M.; Lu, K.; Han, N. M.; Baek, Y.; Chang, C. S.; Suh, J. M.; et al. Graphene nanopattern as a universal epitaxy platform for single-crystal membrane production and defect reduction. *Nat. Nanotechnol.* **2022**, *17* (10), 1054−1059.
(63) Xu, Y.; Cao, B.; He, S.; Qi, L.; Li, Z.; Cai, D.; Zhang, Y.; Ren, G.; Wang, J.; Wang, C.; Xu, K. Evolution of threading dislocations in GaN epitaxial laterally overgrown on GaN templates using self-organized graphene as a nano-mask. *Appl. Phys. Lett.* **2017**, *111* (10), 102105.
(64) Calizo, I.; Bejenari, I.; Rahman, M.; Liu, G.; Balandin, A. A. Ultraviolet Raman microscopy of single and multilayer graphene. *J. Appl. Phys.* **2009**, *106* (4), 043509.
(65) Ferrari, A. C.; Meyer, J. C.; Scardaci, V.; Casiraghi, C.; Lazzeri, M.; Mauri, F.; Piscanec, S.; Jiang, D.; Novoselov, K. S.; Roth, S.; Geim, A. K. Raman spectrum of graphene and graphene layers. *Phys. Rev. Lett.* **2006**, *97* (18), 187401.
(66) Hiramatsu, K.; Amano, H.; Akasaki, I.; Kato, H.; Koide, N.; Manabe, K. MOVPE growth of GaN on a misoriented sapphire substrate. *J. Cryst. Growth* **1991**, *107* (1−4), 509−512.
(67) Metzger, T.; Hopler, R.; Born, E.; Ambacher, O.; Stutzmann, M.; Stommer, R.; Schuster, M.; Gobel, H.; Christiansen, S.; Albrecht, M.; Strunk, H. P. Defect structure of epitaxial GaN films determined

https://doi.org/10.1021/acs.nanolett.4c01724
Nano Lett. 2024, 24, 7458−7466

by transmission electron microscopy and triple-axis X-ray diffractometry. *Philos. Mag (Abingdon)* **1998**, *77* (4), 1013−1025.

https://doi.org/10.1021/acs.nanolett.4c01724
Nano Lett. 2024, 24, 7458−7466